

# Thermophysical properties and thermodynamic phase behavior of ionic liquids<sup>☆</sup>

Urszula Domańska\*

Physical Chemistry Division, Faculty of Chemistry, Warsaw University of Technology, Noakowskiego 3, 00-664 Warsaw, Poland

Received 25 March 2006; received in revised form 23 June 2006; accepted 23 June 2006

Available online 30 June 2006

## Abstract

The thermal stability of many tested ionic liquids (ILs) was investigated by the TGA and DTA curves over the wide temperature range from 200 to 780 K. The TGA curves have mainly a sigmoid shape, which can be split into three segments. The thermal decomposition of the samples was higher than 500 K. For the ammonium salts,  $C_2BF_4$ , or  $C_2PF_6$ , or  $C_2N(CN)_2$ , or  $C_4Br$ , the temperatures of the decompositions were 583.5, 556.1, 545.1 and 525.3 K, respectively. Generally, it was found that the temperature of decomposition of investigated ionic liquid is strongly depended on the type of cation and the anion. Phase equilibria and thermophysical constants were measured also for the dialkoxy-imidazolium ILs,  $[(C_4H_9OCH_2)_2IM][BF_4]$ ,  $[(C_8H_{17}OCH_2)_2IM][Tf_2N]$ ,  $[(C_{10}H_{21}OCH_2)_2IM][Tf_2N]$  and for pyridinium IL,  $[Pyr][BF_4]$ .

The characterization and purity of the compounds were obtained by the elemental analysis, water content (Fisher method) and differential scanning calorimetry (DSC) analysis. From (DSC) method, the melting points, the enthalpies of fusion, the temperatures and enthalpies of solid–solid phase transitions and the half  $C_p$  temperatures of glass transition of all investigated ionic liquids were measured.

The phase equilibria of these salts with common popular solvents: water, or alcohols or *n*-alkanes, or aromatic hydrocarbons have been measured by a dynamic method from 290 K to the melting point of IL, or to the boiling point of the solvent in the whole mole fraction range,  $x$  from 0 to 1.

These salts mainly exhibit simple eutectic systems with immiscibility in the liquid phase with upper critical solution temperatures (UCST), not only with aromatic hydrocarbons, cycloalkanes and *n*-alkanes but also with longer chain alcohols. For example the  $C_2BF_4$  salt show simple eutectic system with water and simple eutectic systems with immiscibility in the liquid phase with upper critical solution temperature with alcohols.

The solid–liquid phase equilibria, SLE curves were correlated by means of the different  $G^{Ex}$  models utilizing parameters derived from the SLE. The root-mean-square deviations of the solubility temperatures for all calculated data depend on the particular system and the equation used.

© 2006 Published by Elsevier B.V.

**Keywords:** Ionic liquids; Thermal stability; Liquid–liquid equilibria; Solid–liquid equilibria

## 1. Introduction

Ionic liquids (ILs) are new generation of solvents for catalysis and synthesis which have been demonstrated as possible new successful replacements for conventional media in new technologies. The important properties include high heat capacity, high density, extremely low volatility, non-flammability, high thermal stability, wide temperature range for liquid, many variations in compositions, and large number of possible variations in cation and anion conformation allowing fine-tuning of the ionic liquid properties for specific applications [1–10]. ILs with their promising physical and chemical properties are

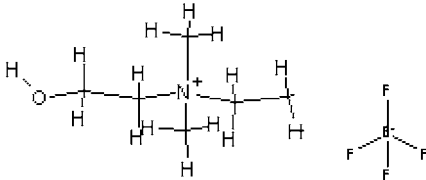
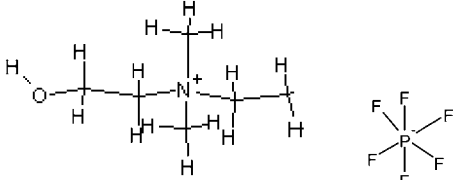
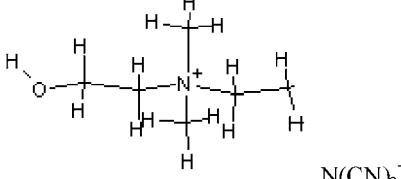
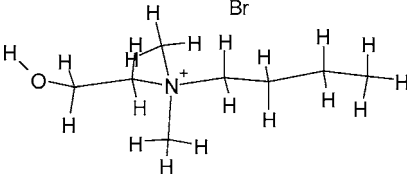
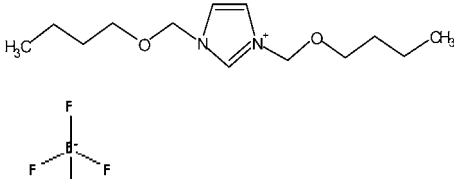
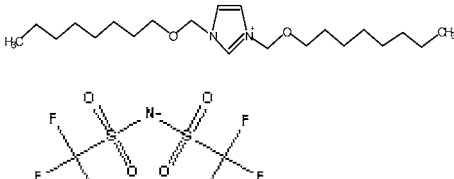
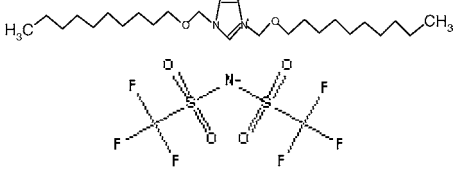
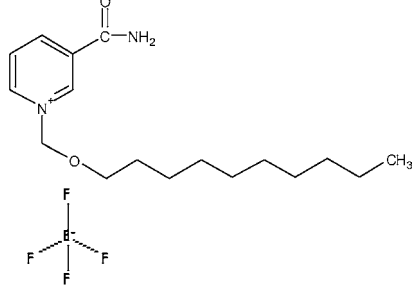
versatile electrolytes for diverse technologies, e.g. in batteries, photoelectrical cells and other electrochemical devices [11–15]. Physical and thermodynamic properties and constants, transport properties, miscibility, and purity assessment were highlighted as immediate needs. The solid–liquid and liquid–liquid phase equilibria measurements of ILs systems based on ammonium cations, or on *N,N'*-dialkyl-substituted imidazolium cations are attracting increasing attention for applications in liquid–liquid extraction [10,16–19]. There are first publications about the suitability of ionic liquids as entrainers for the extractive distillation and as extraction solvents for the liquid–liquid extraction. ILs were found to be capable of breaking a multitude of azeotropic systems. The non-volatility of IL in combination with their remarkable separation efficiency and selectivity enable new processes for the separation of azeotropic mixtures which, in comparison to conventional separation processes, might offer a potential for cost-savings. Until now, it cannot be predicted

<sup>☆</sup> Plenary lecture at the Second International Symposium on Calorimetry and Chemical Thermodynamics, São Pedro, Brazil, 9–13 April 2006.

\* Tel.: +48 22 6213115; fax: +48 22 6282741.

E-mail address: [ula@ch.pw.edu.pl](mailto:ula@ch.pw.edu.pl).

Table 1  
List of ionic liquids investigated in this work

Ethyl-(2-hydroxyethyl)-dimethyl-ammonium tetrafluoroborate		$C_2BF_4$
Ethyl-(2-hydroxyethyl)-dimethyl-ammonium hexafluoroborate		$C_2PF_6$
Ethyl-(2-hydroxyethyl)-dimethyl-ammonium dicyanamide		$C_2N(CN)_2$
Butyl-(2-hydroxyethyl)-dimethyl-ammonium bromide		$C_4Br$
1,3-Dibutyloxymethyl-imidazolium tetrafluoroborate		[[C <sub>4</sub> H <sub>9</sub> OCH <sub>2</sub> ] <sub>2</sub> IM][BF <sub>4</sub> ]
1,3-Dioctyloxymethyl-imidazolium bis(trifluoromethylsulfonyl)imide		[[C <sub>8</sub> H <sub>17</sub> OCH <sub>2</sub> ] <sub>2</sub> IM] [(CF <sub>3</sub> SO <sub>2</sub> ) <sub>2</sub> N] = [Tf <sub>2</sub> N]
1,3-Didecyloxymethyl-imidazolium bis(trifluoromethylsulfonyl)imide		[[C <sub>10</sub> H <sub>21</sub> OCH <sub>2</sub> ] <sub>2</sub> IM] [(CF <sub>3</sub> SO <sub>2</sub> ) <sub>2</sub> N] = [Tf <sub>2</sub> N]
N-Decyloxymethyl-3-amido-pyridinium tetrafluoroborate		[Pyr][BF <sub>4</sub> ]

which IL is the best ones for certain applications. Some ILs as 1-ethyl-3-methyl-imidazolium bis(trifluoromethylsulfonyl)imide, [EMIM][Tf<sub>2</sub>N], or 1-ethyl-3-methyl-imidazolium ethyl sulfate, [EMIM][EtOSO<sub>3</sub>] are excellent entrainers for the separation of aliphatic from aromatic hydrocarbons by extractive distillation or extraction [10,20,21]. The activity coefficients at infinite dilution,  $\gamma_{13}^{\infty}$ , [where 1 refers to the solute (*n*-alkanes, aromatic hydrocarbons, alcohols) and 3 to the solvent (ILs)], provide a useful tool for solvent selection in extractive distillation or solvent extraction processes. Many data was published during the last few years for aliphatic and aromatic hydrocarbons, alcohols and different polar solvents as solutes in ionic liquids ([20–23] and the literature cited in). It was shown for example that 1-butyl-3-methyl-imidazolium octylsulfate, [BMIM][OcOSO<sub>3</sub>] should not be considered as a solvent for separation of alkanes and aromatics [23]. On the other side, two salts as 1,3-dimethyl-imidazolium methoxy ethyl sulfate, [MMIM][CH<sub>3</sub>OC<sub>2</sub>H<sub>4</sub>OSO<sub>3</sub>] and 4-methyl-*n*-butyl-pyridinium tetrafluoroborate, [BMPYR][BF<sub>4</sub>] were found to exhibit very high selectivity for hexane/benzene separation [24,25]. Generally, the separation of the aliphatic/aromatic hydrocarbons decreases with an increasing length of the alkyl chain at the cation, or anion of IL.

To design any process involving ionic liquids on an industrial scale it is necessary to know phase equilibria and especially liquid–liquid equilibrium [26–37] and solid–liquid equilibrium [38–42].

In most of the published papers the liquid–liquid equilibrium between alcohols and ILs have been studied and the partitioning of alcohols between ionic liquids and water was described. In general, (ILs + an alcohol) binary mixtures show LLE with upper critical points shifted to the alcohol higher mole fraction. An increase in the alkyl chain length of the alcohol resulted in an increase in the UCST. Branching of the alcohol resulted in a higher solubility of the alcohol in the IL-rich phase. By increasing the alkyl chain length on the imidazolium ring, the UCST decreased. The replacement of the hydrogen at C<sub>2</sub> position of the ring with the methyl group resulted in an increase in the UCST [29].

In our previous work the solubility of 1-ethyl-3-methyl-imidazolium hexafluorophosphate, [EMIM][PF<sub>6</sub>], or 1-butyl-3-methyl-imidazolium hexafluorophosphate, [BMIM][PF<sub>6</sub>], in aromatic hydrocarbons, or in *n*-alkanes, or in cyclohydrocarbons, or in alcohols has been measured [31,32]. In many cases the observation of the upper critical solution temperature was limited by the boiling temperature of the solvent. The solubility of [EMIM][PF<sub>6</sub>] and [BMIM][PF<sub>6</sub>] in aromatic hydrocarbons and in alcohols decreases with an increase of the molecular weight of the solvent.

The recently published study on solutions of 1,3-dimethyl-imidazolium methylsulfate, [MMIM][CH<sub>3</sub>SO<sub>4</sub>] and 1-butyl-3-methylimidazolium methylsulfate, [BMIM][CH<sub>3</sub>SO<sub>4</sub>] with aromatic hydrocarbons, or with *n*-alkanes, or with cyclohydrocarbons, or with alcohols have presented useful from the technological perspective properties, because they have shown partial immiscibility at room temperature [36,37]. By increasing the alkyl chain length on the cation, the upper critical solution temperature, UCST decreased in all solvents except in *n*-alkanes.

Also the choice of anion was shown to have large impact on the UCST of the systems of 1-hexyloxymethyl-3-methyl-imidazolium-based ILs with the anions [BF<sub>4</sub>]<sup>−</sup> and [Tf<sub>2</sub>N]<sup>−</sup>; the solubility dramatically increased and the UCST decreased for the [Tf<sub>2</sub>N]<sup>−</sup> anion [34].

This paper follows the discussion on room temperature ionic liquids, and is a continuation of our systematic study of the impact of different factors on the phase behavior of alkyl-(2-hydroxyethyl)-dimethyl-ammonium cation [C<sub>*n*</sub>] with different anions [Br<sup>−</sup>, or BF<sub>4</sub><sup>−</sup>, or PF<sub>6</sub><sup>−</sup>, or N(CN)<sub>2</sub><sup>−</sup>] and of 1,3-dialkoxymethyl-imidazolium ((C<sub>*n*</sub>H<sub>2*n*</sub>OCH<sub>2</sub>)<sub>2</sub>IM<sup>+</sup>) cations with different anions [BF<sub>4</sub><sup>−</sup>, or Tf<sub>2</sub>N<sup>−</sup>] with benzene and alcohols. This work focused on understanding what features control the LLE and SLE phase equilibrium of ammonium and imidazolium-based ionic liquids with different organic solvents. Characteristic investigated here include the effect of anion {[BF<sub>4</sub><sup>−</sup>] versus [Br<sup>−</sup>]} in alkyl-(2-hydroxyethyl)-dimethyl-ammonium salts; the effect of the alkyl chain length (butyl versus ethyl) of the cation at ammonium salts; the effect of the alkyl chain length of the cation (butyl- versus octyl-, or decyl-) in the 1,3-dialkoxymethyl-imidazolium salts; the effect of the pyridinium ring versus imidazolium ring in the cation. The names of substances under study, chemical formulas and the abbreviations are presented in Table 1.

The melting point, the glass transition temperature, enthalpy of fusion, and enthalpy of solid–solid phase transition were determined by the differential scanning calorimetry, DSC and the decomposition by the TG/DTA for most of the ionic liquids under study.

The determination of the IL–solvent interaction of these salts via the solubility measurements especially with water, or alcohols, or benzene, or *n*-hydrocarbons, or cyclohydrocarbons have been performed. The characterization and purity of the compounds were obtained by the elemental analysis, water content (Fisher method), differential scanning microcalorimetry (DSC) analysis and by (TG/DTA) analysis.

For a better understanding of the IL behavior and with a view to the application in chemical engineering or the development of thermodynamic models, reliable experimental data are required. Basic IL can act as both a hydrogen bond acceptor (anion) and donor (cation) and would be expected to interact with solvents with both accepting and donating sites. On the other hand, polar solvents as alcohols are very well-known to form hydrogen-bonded net with both high enthalpies and constants of association. In this work the higher interaction may be expect between hydroxyl group of ammonium salt, or dialkoxy-group with polar solvent as water, or alcohol. The better solubility of IL in a chosen solvent means the possible hydrogen bonding between IL and solvent.

## 2. Experimental

### 2.1. Materials

1. Investigated alkyl-(2-hydroxyethyl)-dimethyl-ammonium compounds were synthesized using the *N,N*-dimethylethanolamine (Sigma–Aldrich CAS number 108-01-0) and appro-

Table 2  
Thermophysical constants of pure ammonium salts, determined from DSC data<sup>a</sup>

Compound	$T_{\text{fus},1}$ (K)	$\Delta_{\text{fus}}H_1$ (kJ mol <sup>-1</sup> )	$T_{\text{tr},1}$ (K)	$\Delta_{\text{tr}}H_1$ (kJ mol <sup>-1</sup> )	$T_{\text{dec},1}$ (K)
C <sub>2</sub> BF <sub>4</sub>	426.8	5.14	311.5; 252.8; 146 (g) <sup>b</sup>	1.17; 3.06	583.5
C <sub>2</sub> PF <sub>6</sub>	272.0	10.60	–	–	556.1
C <sub>2</sub> N(CN) <sub>2</sub>	282.7	8.60	168.4 (g) <sup>c</sup>	–	545.1
C <sub>4</sub> Br <sup>a</sup>	359.3	13.21	187.3 (g) <sup>d</sup>	–	525.3

<sup>a</sup> Data for C<sub>2</sub>Br, C<sub>3</sub>Br, C<sub>4</sub>Br, C<sub>6</sub>Br were published earlier [41].

<sup>b</sup>  $\Delta C_p$  at the glass transition is equal to 20.0 J mol<sup>-1</sup> K<sup>-1</sup>.

<sup>c</sup>  $\Delta C_p$  at the glass transition is equal to 16.7 J mol<sup>-1</sup> K<sup>-1</sup>.

<sup>d</sup>  $\Delta C_p$  at the glass transition is equal to 30.9 J mol<sup>-1</sup> K<sup>-1</sup>.

priate haloalkane such as: ethyl bromide (Sigma–Aldrich CAS number 74-96-4), or butyl bromide (Sigma–Aldrich CAS number 109-65-9). Substances were placed into round bottom flask and were mixed in 10% excess of haloalkane. The intermediates were heated at 353 K for 30 min and stirred under reflux to form the reaction mixture. After that, mixture was cooled down and the obtained solid product was dissolved in mixture of 1-propanol (Sigma–Aldrich CAS number 71-23-8) and methanol (Sigma–Aldrich CAS number 67-56-1) at ratio 1:3. Subsequently, the mixture was heated at 353 K for 30 min under reflux. Later, mixture was cooled down and cyclohexane (Sigma–Aldrich CAS number 110-82-7) in very small portion was added into the mixture to form the solid powder. Solid phase was filtered through the S<sub>4</sub> filter and that phase was collected. To the liquid phase, next portion of cyclohexane was added to the completely give off the product. All salts were recrystallised from mixture of 1-propanol and methanol and then rigorously dried under vacuum for 48 h prior to use. We believe that the solvents and unreacted reagents were removed under vacuum from white solid, which was obtained with yield higher than 88%. The compounds were characterized using FTIR, NMR, mass spectroscopy, and elemental analysis. The brief characterization of obtained compounds was presented in our previous work [41]. The physicochemical constants are presented in Table 2.

2. The imidazolium ILs were synthesized: the 1,3-dialkoxyloxymethyl-imidazolium tetrafluoroborate ([BF<sub>4</sub><sup>-</sup>]), or bis-(trifluoromethylsulfonyl)imide ([CF<sub>3</sub>SO<sub>2</sub>)<sub>2</sub>N<sup>-</sup>] = [Tf<sub>2</sub>N]) were obtained from 1,3-alkoxymethyl-imidazolium chloride [43,44]. The prepared ILs were characterized by their <sup>1</sup>H NMR and <sup>13</sup>C NMR spectra. <sup>1</sup>H NMR spectra were recorded on a Varian Model XL 300 spectrometer at 300 MHz with tetramethylsilane as the standard. <sup>13</sup>C NMR spectra were

recorded on the same instrument at 75 MHz to confirm of any major impurities. All ionic liquids were cleaned with activated carbon to remove any colored compounds and dried under vacuum at 348.15 K for 48 h to remove organic solvents and water. Analysis for the water contamination using the Karl–Fischer technique for solvents and ILs showed that the impurity in each of the substances was <0.02 mol%. The physicochemical properties of imidazolium and pyridinium ionic liquids discussed in this work are presented in Table 3.

All solvents were delivered from Sigma–Aldrich Chemie GmbH, Stenheim, Germany. Before direct use they were fractionally distilled over different drying reagents to the mass fraction purity  $\geq 99.8$  mass%. The solvents were stored over freshly activated molecular sieves of type 4 Å (Union Carbide).

## 2.2. Methods

### 2.2.1. Water content

Water content was analyzed by Karl–Fischer titration technique (method TitroLine KF). Samples of all compounds were dissolved in methanol and titrated with step 2.5  $\mu$ l. The results show water content from 170 to 300 ppm.

### 2.2.2. Differential scanning microcalorimetry (DSC)

The melting point, the enthalpy of fusion and the enthalpy of the solid–solid phase transition of every salt were measured using a differential scanning microcalorimetry (DSC) at the 5 K min<sup>-1</sup> scan rate with the power sensitivity of 16 mJ s<sup>-1</sup> and with the recorder sensitivity of 5 mV. The instrument (Perkin-Elmer Pyris 1) was each time calibrated with the 99.9999 mol% purity indium sample. The calorimetric accuracy was  $\pm 1\%$

Table 3  
Thermophysical constants of pure imidazolium salts and pyridinium salt, determined from DSC data

Compound	$T_{\text{fus},1}$ (K)	$\Delta_{\text{fus}}H_1$ (kJ mol <sup>-1</sup> )	$T_{\text{tr},1}$ (K)	$\Delta_{\text{tr}}H_1$ (kJ mol <sup>-1</sup> )
[(C <sub>4</sub> H <sub>9</sub> OCH <sub>2</sub> ) <sub>2</sub> IM][BF <sub>4</sub> ]	281.4	8.54	267.4	10.86
[(C <sub>8</sub> H <sub>17</sub> OCH <sub>2</sub> ) <sub>2</sub> IM][Tf <sub>2</sub> N]	287.7	34.20	–	–
[(C <sub>10</sub> H <sub>21</sub> OCH <sub>2</sub> ) <sub>2</sub> IM][Tf <sub>2</sub> N]	303.1	79.36	–	–
[Pyr][BF <sub>4</sub> ]	361.9	51.26	–	–

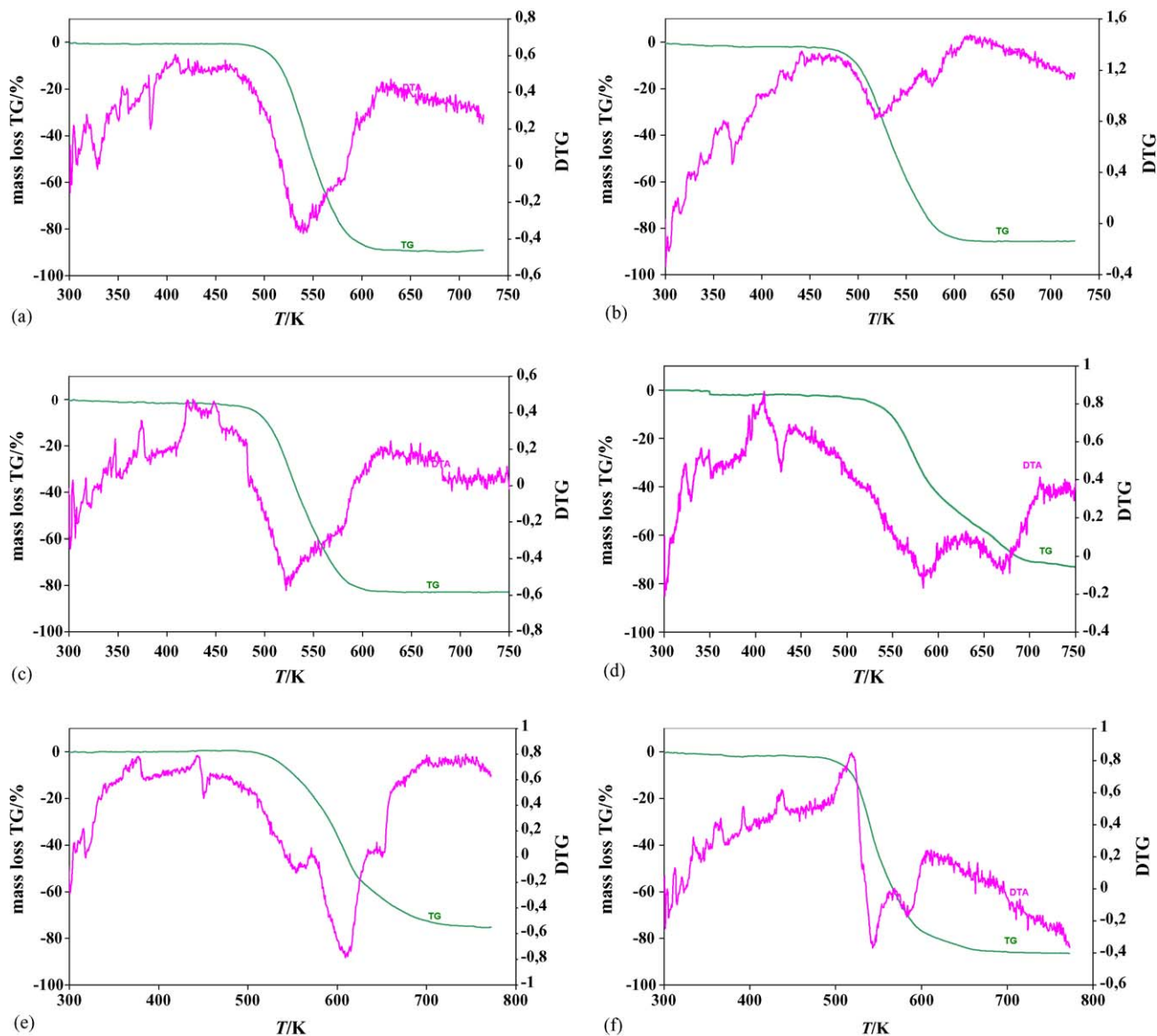


Fig. 1. Thermogravimetric analysis (TGA) curves of the thermal degradation and decomposition (DTG)–[d(mass loss)/dT] curves of the thermal degradation of ammonium salts: (a)  $C_3Br$ ; (b)  $C_4Br$ ; (c)  $C_6Br$ ; (d)  $C_2BF_4$ ; (e)  $C_2PF_6$ ; (f)  $C_2N(CN)_2$ .

and the calorimetric precision was  $\pm 0.5\%$ . The thermophysical properties are shown in Tables 2 and 3.

### 2.2.3. Decomposition of compounds

Simultaneous TG/DTA experiments were performed using a MOM Derivatograph, PC (Hungary). In general, runs were carried out using matched labyrinth platinum crucibles with  $Al_2O_3$  in reference pan. The crucible design hampered the migration of volatile decomposition products reducing the rate of gas evolution and, in turn, increasing contact time of the reactants. All TG/DTA curves were obtained at  $5\text{ K min}^{-1}$  heating rate with a nitrogen dynamic atmosphere (flow rate  $20\text{ dm}^3\text{ h}^{-1}$ ). Temperatures of decomposition, obtained from the first minimum of the DTA curves for the ammonium salts are presented as an example in Table 2. Figs. 1 and 2 present the comparison of decomposition (mass loss) and DTA for chosen salt.

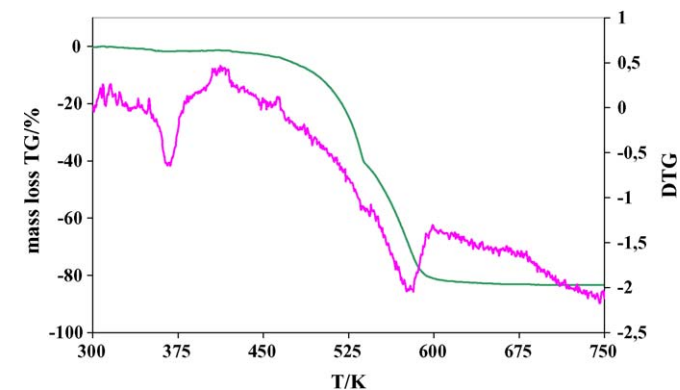


Fig. 2. Thermogravimetric analysis (TGA) curves of the thermal degradation and DTG of the pyridinium salt,  $[Pyr][BF_4]$ .

### 2.2.4. Solid–liquid and liquid–liquid equilibria apparatus measurements

Solid–liquid equilibrium, SLE and liquid–liquid equilibrium, LLE temperatures were determined using a dynamic method described in detail previously [34–42]. Appropriate mixtures of solute and solvent placed under the nitrogen in dry box into a Pyrex glass cell were heated very slowly (less than  $2\text{ K h}^{-1}$  near the equilibrium temperature) with continuous stirring inside a cell which was placed in a glass thermostat filled with silicone oil, or water. The temperature of the liquid bath was varied slowly until the last crystals disappeared. This temperature was taken as the temperature of the solid–liquid equilibrium in the saturated solution. The crystal disappearance temperatures were detected visually. In LLE measurements a sample of known composition was placed in a view-cell and heated until it was one phase. The equilibrium temperature was two phases (foggy mixture) disappearance in the liquid phase, observed visually during increasing temperature. The observation of the “cloud point” with decreasing temperature was very difficult. The effect of precooling and kinetics of the phenomenon of binary phases creation were the reasons that the temperature of “cloud point” was not repeatable during the experiment. The temperature was measured with an electronic thermometer P 550 (DOSTMANN electronic GmbH) with the probe totally immersed in the thermostating liquid. The accuracy of the temperature measurements was judged to be  $\pm 0.01\text{ K}$ . Mixtures were prepared by mass and the uncertainty in the composition was estimated to be  $\pm 0.0005$  and  $\pm 0.5\text{ K}$  in the mole fraction and temperature, respectively. It was found that the solution–crystallization procedure was quite slow and difficult, thus the solubility measurements were very time-consuming. The LLE measurements were limited at the upper temperature by the boiling point of the solvent, or the possible maximum temperature of the experiment (oil bath).

## 3. Results

### 3.1. Thermal decomposition

Received salts demonstrate high temperature of decomposition. For investigated components the temperature of decomposition strongly depends on the alkyl chain length. In ammonium bromide salts for the shortest alkyl chain in the cation, the temperature of decomposition is the highest and equals  $559.3\text{ K}$  for  $\text{C}_2\text{Br}$  [41]. For the longer alkyl chain, the temperature of decomposition decreases to  $525.37\text{ K}$  for  $\text{C}_4\text{Br}$ , what is presented in Fig. 1. Compounds have been decomposed in one step. The percent of mass loss of ionic liquids decreases with increasing of alkyl chain length. The highest value equals to 92.25% was obtained for  $\text{C}_2\text{Br}$  and the lowest for  $\text{C}_6\text{Br}$  (does not exceed 82.8%) [41]. Changing the anion for the same cation, e.g. ethyl-(2-hydroxyethyl)-dimethyl-ammonium ( $\text{C}_2$ ) causes the decreasing of the first step decomposition temperature  $10\text{--}30\text{ }^\circ\text{C}$ . The lowest first step decomposition temperature,  $545.1\text{ K}$  was found for  $\text{C}_2\text{N}(\text{CN})_2$ . Thermogravimetric analysis (TGA) curves of the thermal degradation and DTA of the alkoxy-imidazolium salts have shown the decomposition temperature about  $500\text{ K}$ . For the longer alkyl chain the temperature of decomposition increases

(contrary to ammonium salts). For pyridinium salt the decomposition temperature is  $580\text{ K}$  (see Fig. 2).

DSC diagram for  $\text{C}_4\text{Br}$  presents the melting point at  $359.3\text{ K}$ , what is much lower in comparison with  $\text{C}_2\text{Br}$  ( $541.4\text{ K}$ ) [41]. The melting temperatures of the other  $\text{C}_2$  ammonium salts are presented in Table 2. Only  $\text{C}_2\text{BF}_4$  salt melts higher than  $420\text{ K}$ .

Fortunately, the imidazolium salts exhibit lower melting temperatures, what is shown in Table 3. The lowest melting temperature was observed for  $[(\text{C}_4\text{H}_9\text{OCH}_2)_2\text{IM}][\text{BF}_4]$   $T = 281.44\text{ K}$ . Only the pyridinium salt  $[\text{Pyr}][\text{BF}_4]$  melts at high temperature,  $T = 360.12\text{ K}$ . Melting temperature of the solute, its enthalpy of melting and the interaction between solute and solvent are responsible for the solubilities, SLE and LLE presented in the next chapter.

### 3.2. Phase diagrams

Experimental phase diagrams of SLE investigated in this work are not easy for the interpretation, inherently because solutes are very complicated and highly interacting molecules, especially in water and alcohols. For this discussion, the chosen solid–liquid equilibria for new binary ionic liquid–organic solvent systems were determined. As an example of ammonium salts the solubilities of  $\text{C}_2\text{BF}_4$  in water, or butan-1-ol, or butan-2-ol, or octan-1-ol, or dodecan-1-ol and of  $\text{C}_4\text{Br}$  in hydrocarbons (hexane, or heptane, or cyclohexane) were measured and compared with previously measured  $\text{C}_2\text{Br}$  in alcohols [42] and  $\text{C}_2\text{Br}$ , or  $\text{C}_3\text{Br}$ , or  $\text{C}_4\text{Br}$ , or  $\text{C}_6\text{Br}$  in water and octan-1-ol [41]. The results of ammonium salts are summarized in Table 1S ( $\text{C}_2\text{BF}_4$ ) and Table 2S ( $\text{C}_4\text{Br}$ ). Phase diagrams are presented in Figs. 3–6.

The ability of a polar cation to create the hydrogen bond with water, or an alcohol significantly increases the solubilities of IL

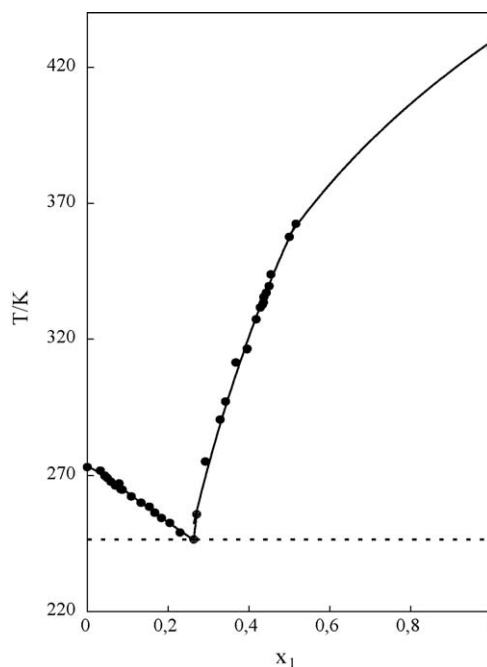


Fig. 3. Solid–liquid equilibrium diagram of  $[\text{C}_2\text{BF}_4 (1) + \text{water} (2)]$  binary system; full lines drawn to guide the eye.

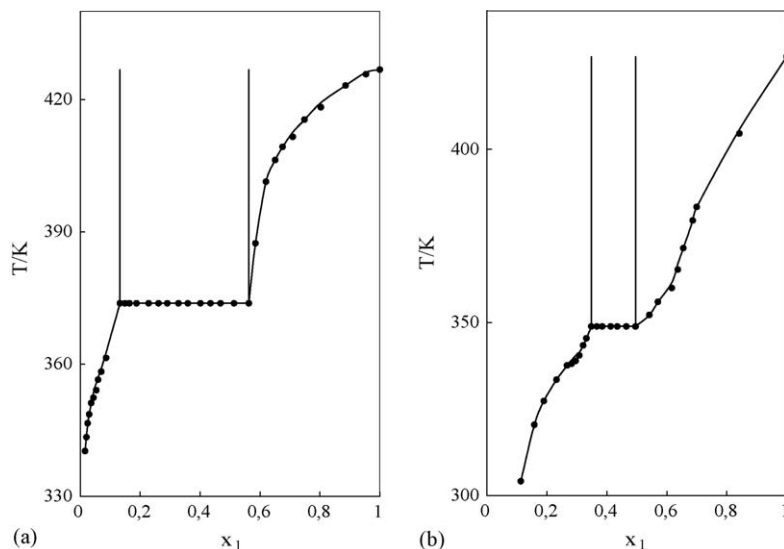


Fig. 4. Solid–liquid equilibrium diagrams of binary systems: (a)  $[C_2BF_4 (1) + \text{butan-1-ol} (2)]$ ; (b)  $[C_2BF_4 (1) + \text{butan-2-ol} (2)]$ ; full lines drawn to guide the eye.

in these solvents. The interaction of hydroxyl group,  $[OH^-]$  of cation with water is so strong that full miscibility was observed for  $C_nBr$  (where  $n = 2-4, 6$ ), with water [41], and of  $C_2BF_4$  with water (see Fig. 3). Changing the anion  $[Br^-]$  for  $[BF_4^-]$  the decrease of the melting temperature of the IL was observed, what resulted in better solubility of  $C_2BF_4$  in water (see [41] and Table 1S). The eutectic point of  $(C_2BF_4 + \text{water})$  system is shifted to the lower solute mole fraction ( $T_{1,e} = 246.0 \text{ K}$ ,  $x_{1,e} = 0.2631$ ) (see Fig. 3). For the  $C_2Br$  the eutectic point was  $T_{1,e} = 248.1 \text{ K}$ ,  $x_{1,e} = 0.3575$  [41].

The effect of interaction with alcohols is different for  $C_2Br$  and  $C_2BF_4$ . The solubility of  $C_2Br$  in alcohols from ethanol to dodecan-1-ol did not present the miscibility gap [40], whilst  $C_2BF_4$  showed immiscibility in alcohols at high temperatures. These systems exhibit upper critical solution temperature behavior, UCST which is higher than 435 K for every system measured

(see Figs. 4 and 5). The solubility (solute mole fraction) of  $C_2BF_4$  in alcohols at 323.15 K is  $1 \times 10^{-3}$ , 0.173,  $1 \times 10^{-3}$  in butan-1-ol, butan-2-ol and dodecan-1-ol, respectively. In the secondary alcohol the higher solute–solvent interaction was observed.

The influence of the cation's alkyl chain length was observed previously for  $C_nBr$  (where  $n = 2-4, 6$ ), on the melting temperature of ammonium salts [41]. The decrease in the melting temperature of the salt was observed with an increase of the alkyl chain length of the cation. For different anions and ethyl substituent at the nitrogen of ammonium salt, the melting temperature decreases and make possible to measure the SLE for  $C_2BF_4$  with hydrocarbons: hexane, heptane and cyclohexane. Fig. 5 presents the solubility of  $C_2BF_4$  in heptane and cyclohexane as an example. Usually, the UCST increases as the length of the alkyl chain of the hydrocarbon increases. This trend was observed

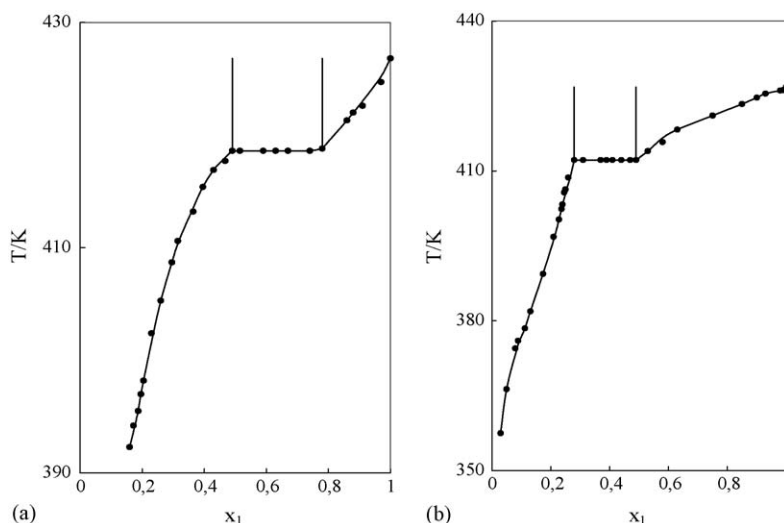


Fig. 5. Solid–liquid equilibrium diagrams of binary systems: (a)  $[C_2BF_4 (1) + \text{octan-1-ol} (2)]$ ; (b)  $[C_2BF_4 (1) + \text{dodecan-1-ol}]$ ; full lines drawn to guide the eye.

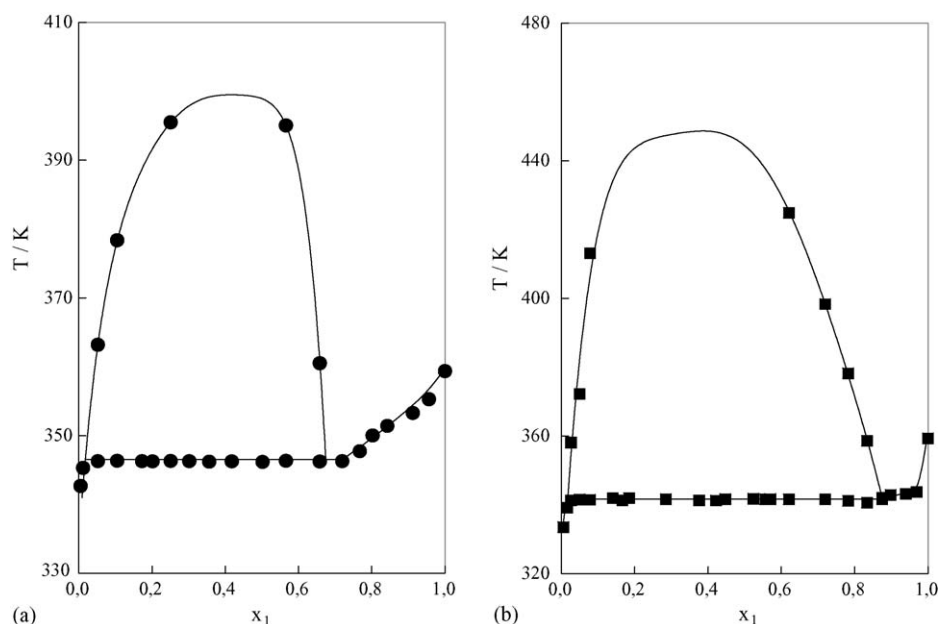


Fig. 6. Solid–liquid and liquid–liquid equilibrium diagrams of binary systems: (a)  $[\text{C}_4\text{Br}$  (1) + heptane (2)]; (b)  $[\text{C}_4\text{Br}$  (1) + cyclohexane (2)]; full lines drawn to guide the eye.

for systems investigated in this work and in our previous study for alkyimidazolium salts as  $[\text{EMIM}][\text{PF}_6]$  and  $[\text{BMIM}][\text{PF}_6]$  [31], or of  $[\text{MMIM}][\text{CH}_3\text{SO}_4]$  and  $[\text{BMIM}][\text{CH}_3\text{SO}_4]$  [36], or of  $[\text{C}_6\text{H}_{13}\text{OCH}_2\text{MIM}][\text{BF}_4]$  [34].

In cyclohexane solubility decreases in comparison with *n*-alkanes; the UCST increases and immiscibility exists in much wider salt mole fraction region. The reason is the chemical structure of the solvent and the solute: cyclohexane as a cyclic molecule cannot “come close” to the alkane chains at the nitrogen atom of ammonium salt. The same effect was observed for  $\text{C}_4\text{Br}$  in heptane and in cyclohexane (see Fig. 6a and b).

The effect of the alkoxy-group of the cation on the solubility of imidazolium IL in different solvents was discussed in our previous paper [34]. The effect of the anion ( $[\text{Tf}_2\text{N}^-]$  versus  $[\text{BF}_4^-]$ ) for  $[\text{C}_6\text{H}_{13}\text{OCH}_2\text{mim}^+]$  cation was discussed. Greater mutual solubilities were observed for  $[\text{C}_6\text{H}_{13}\text{OCH}_2\text{mim}][\text{Tf}_2\text{N}]$  than for  $[\text{C}_6\text{H}_{13}\text{OCH}_2\text{mim}][\text{BF}_4]$  [34]. The best solubility was shown by the  $[\text{C}_6\text{H}_{13}\text{OCH}_2\text{mim}][\text{Tf}_2\text{N}]$  in every solvent. The immiscibility gap for alcohols was usually lower than that in benzene; the solubilities in ethers were comparable with solubilities in cyclohexane and in heptane [34].

In this work the results of the solubility measurements are presented for three dialkoxy-salts:  $[(\text{C}_4\text{H}_9\text{OCH}_2)_2\text{IM}][\text{BF}_4]$ , or  $[(\text{C}_8\text{H}_{17}\text{OCH}_2)_2\text{IM}][\text{Tf}_2\text{N}]$ , or  $[(\text{C}_{10}\text{H}_{21}\text{OCH}_2)_2\text{IM}][\text{Tf}_2\text{N}]$  in alcohols (ethanol, octan-1-ol) and in benzene. The results are presented in Tables 3S–6S and in Figs. 7–12. The second alkoxy-group in the molecule of IL causes the stronger interaction with the solvent. Only the  $[(\text{C}_4\text{H}_9\text{OCH}_2)_2\text{IM}][\text{BF}_4]$  salt with tetrafluoroborate anion exhibit small miscibility gap in alcohols in the IL low mole fraction (the area of immiscibility shifts towards solvent rich region). Much higher binary liquids area was observed in benzene (see Fig. 9). In benzene rather the *n*- $\pi$  interaction exist than hydrogen bonding as it was possible in alcohols. Greater mutual solubilities were observed for bis(trifluoro-

methylsulfonyl)imide anion even for the longer the alkoxy-chains on the cation ( $\text{C}_8$  versus  $\text{C}_4$ ). Complete miscibility in the liquid phase was observed for  $[(\text{C}_8\text{H}_{17}\text{OCH}_2)_2\text{IM}][\text{Tf}_2\text{N}]$ , or  $[(\text{C}_{10}\text{H}_{21}\text{OCH}_2)_2\text{IM}][\text{Tf}_2\text{N}]$  in alcohols (ethanol, octan-1-ol) and in benzene (see Figs. 10–12). The solubility decreases as the molecular weight of the alcohol increases. The eutectic point in binary system of  $\{[(\text{C}_4\text{H}_9\text{OCH}_2)_2\text{IM}][\text{BF}_4]$  (1) + benzene (2) $\}$  was  $T_{1,e} = 260.3 \text{ K}$ ,  $x_{1,e} = 0.450$  and for

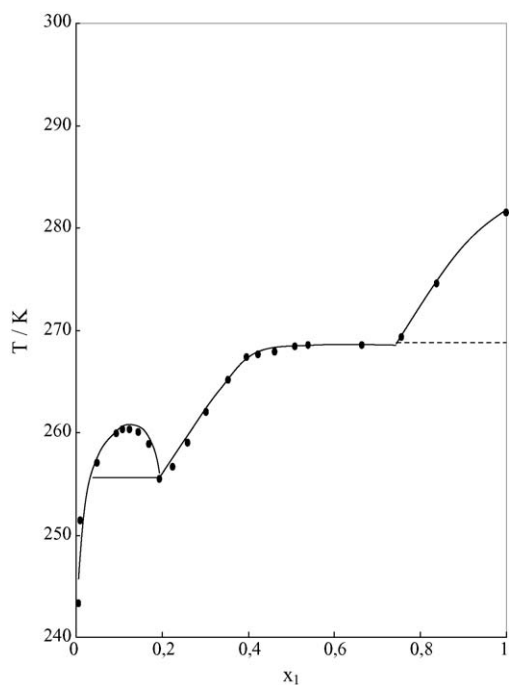


Fig. 7. Solid–liquid and liquid–liquid equilibrium diagram of binary system  $\{[(\text{C}_4\text{H}_9\text{OCH}_2)_2\text{IM}][\text{BF}_4]$  (1) + ethanol (2) $\}$ ; dotted line, solid–solid phase equilibrium temperature; full lines drawn to guide the eye.



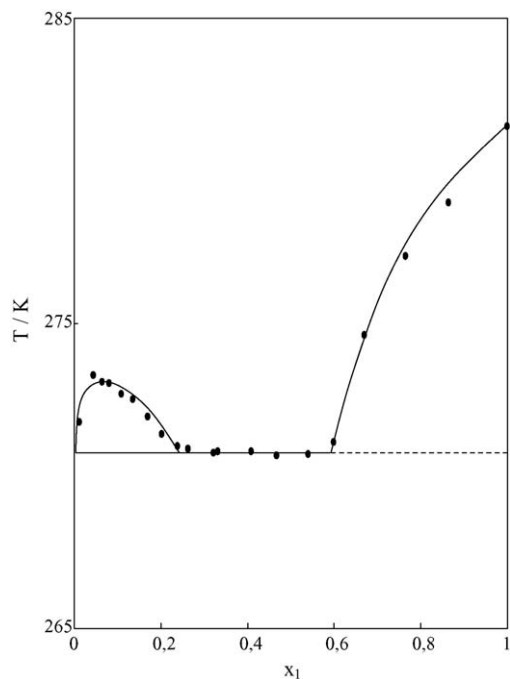


Fig. 8. Solid-liquid and liquid-liquid equilibrium diagram of binary system  $\{[(C_4H_9OCH_2)_2IM][BF_4] (1) + \text{octan-1-ol} (2)\}$ ; dotted line, solid-liquid phase equilibrium temperature; full lines drawn to guide the eye.

binary system  $\{[(C_8H_{17}OCH_2)_2IM][Tf_2N] (1) + \text{benzene} (2)\}$  was  $T_{1,e} = 271.8 \text{ K}$ ,  $x_{1,e} = 0.331$ . In every system with  $[(C_4H_9OCH_2)_2IM][BF_4]$  the solid-liquid phase transition was noted in a phase diagram.

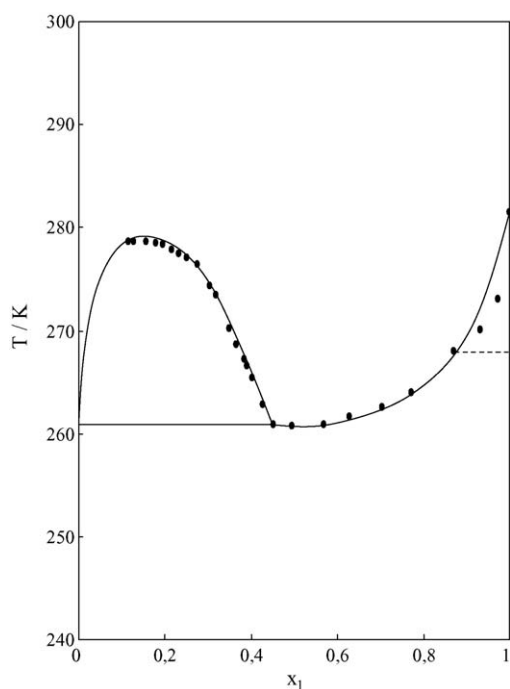


Fig. 9. Solid-liquid and liquid-liquid equilibrium diagram of binary system  $\{[(C_4H_9OCH_2)_2IM][BF_4] (1) + \text{benzene} (2)\}$ ; dotted line, solid-liquid phase equilibrium temperature; full lines drawn to guide the eye.

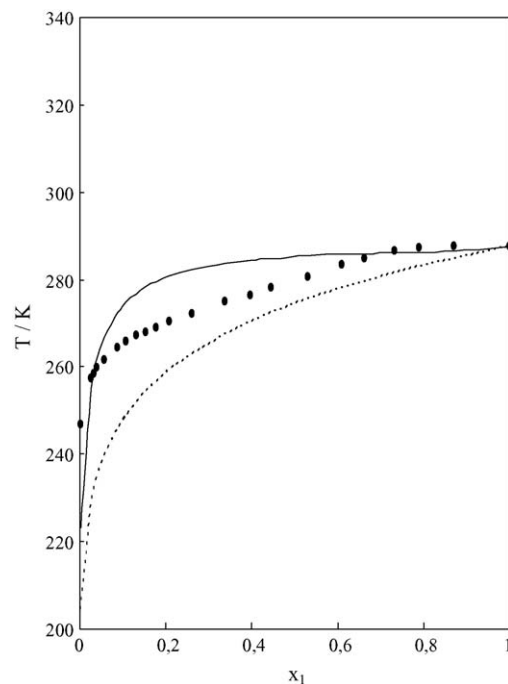


Fig. 10. Solid-liquid equilibrium diagram of binary system  $\{[(C_8H_{17}OCH_2)_2IM][Tf_2N] (1) + \text{ethanol} (2)\}$ ; ●, experimental points; dotted line, ideal solubility; solid line, calculated by the UNIQUAC ASM equation.

The influence of the alkoxy-chain length of cation for two ILs with the same anion can be observed from [Table 3](#) and [Tables 4S–6S](#). The longer alkoxy-chain causes the higher melting temperature of the compound and the lower solubility.

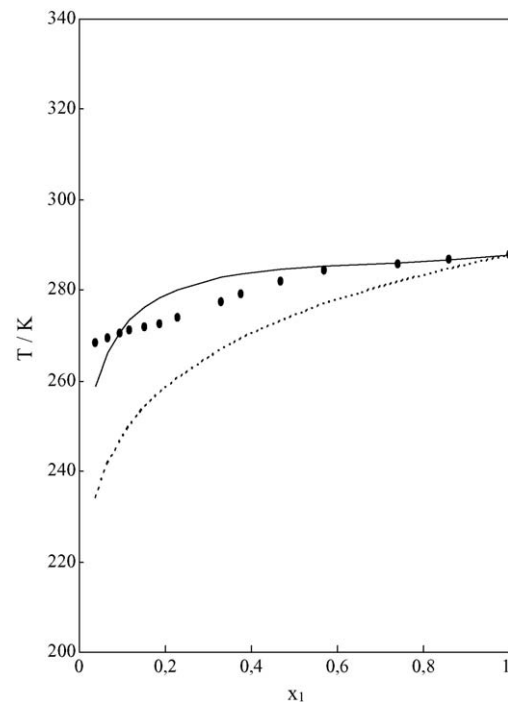


Fig. 11. Solid-liquid equilibrium diagram of binary system  $\{[(C_8H_{17}OCH_2)_2IM][Tf_2N] (1) + \text{octan-1-ol} (2)\}$ ; ●, experimental points; dotted line, ideal solubility; solid line, calculated by the UNIQUAC ASM equation.

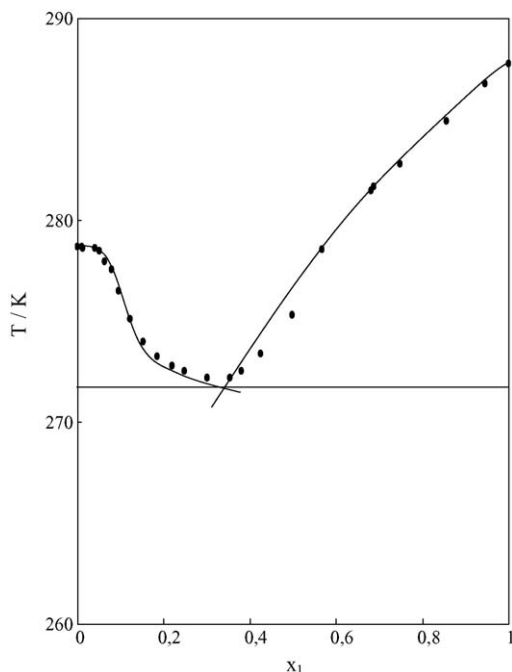


Fig. 12. Solid-liquid equilibrium diagram of binary system  $\{[(C_8H_{17}OCH_2)_2IM][Tf_2N](1) + \text{benzene}(2)\}$ ; full lines drawn to guide the eye.

The influence of the pyridinium ring, or the imidazolium ring on the solubility can be partly discussed from the solubility measurements of *N*-decyloxymethyl-3-amido-pyridinium tetrafluoroborate,  $[Pyr][BF_4]$  in alcohols (ethanol, butan-1-ol, hexan-1-ol, dodecan-1-ol) and in benzene (see Tables 7S–9S). Unfortunately, this compound has only one alkoxy-group and one new amido-group which causes additional interaction with

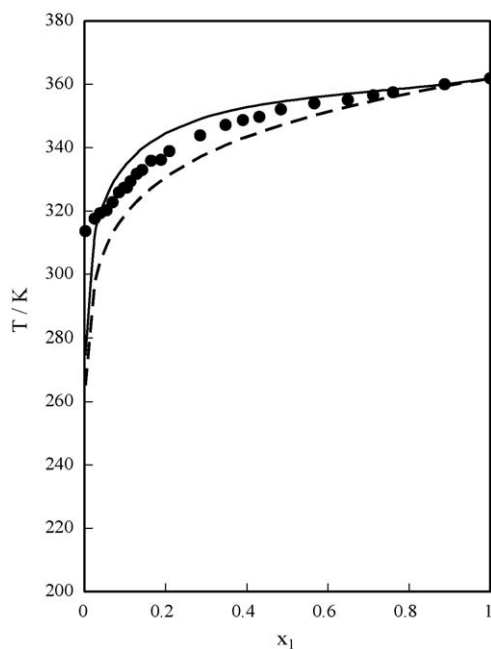


Fig. 13. Solid-liquid equilibrium diagram of binary system  $\{[Pyr][BF_4](1) + \text{ethanol}(2)\}$ ; ●, experimental points; dotted line, ideal solubility; solid line, calculated by the UNIQUAC ASM equation.

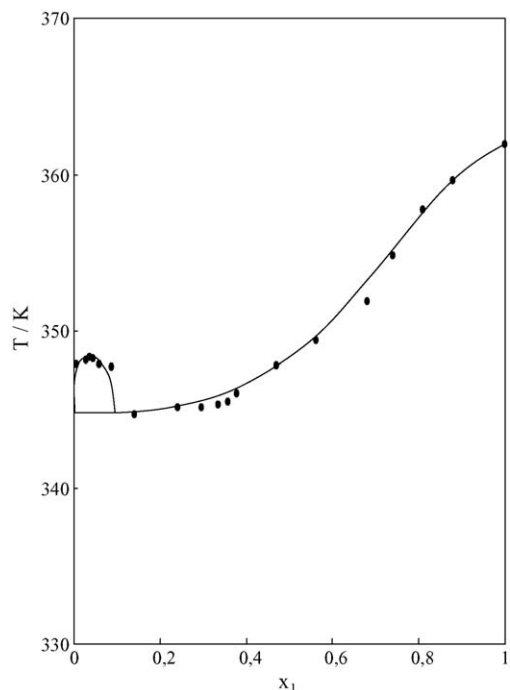


Fig. 14. Solid-liquid and liquid-liquid equilibrium diagram of binary system  $\{[Pyr][BF_4](1) + \text{dodecan-1-ol}(2)\}$ ; dotted line, solid-solid phase equilibrium temperature; full lines drawn to guide the eye.

the solvent. Anyway, the melting temperature is higher than it was observed for the alkoxy-imidazolium salts; the solubility is lower (see for example Fig. 13). Complete miscibility was observed for alcohols with the exception of dodecan-1-ol, for which the small area of immiscibility was observed in low IL mole fraction. The eutectic points in the systems with alcohols are shifted to the very low IL mole fraction (see Fig. 14). Implied eutectic point in binary system  $\{[Pyr][BF_4](1) + \text{benzene}(2)\}$  is  $T_{1,e} = 332.5 \text{ K}$ ,  $x_{1,e} = 0.150$ .

#### 4. Correlation of the experimental data

The data of LLE, obtained for the solvent high mole fraction does not authorize to do any calculations in the area of LLE. In many binary mixtures it was impossible to detect the equilibrium curve at the low IL mole fraction area by the visual method. The observation of the liquid-liquid demixing was inhibited by the permanently foggy solution. The spectroscopic or other techniques are necessary to use in the mixtures under study in the future.

The solid-liquid equilibria in a mixture of a solid 1 in a liquid may be expressed in a very general manner by Eq. (1):

$$-\ln x_1 = \frac{\Delta_{\text{fus}}H_1}{R} \left( \frac{1}{T} - \frac{1}{T_{\text{fus},1}} \right) - \frac{\Delta_{\text{fus}}C_{p,1}}{R} \left( \ln \frac{T}{T_{\text{fus},1}} + \frac{T_{\text{fus},1}}{T} - 1 \right) + \ln \gamma_1 \quad (1)$$

where  $x_1$ ,  $\gamma_1$ ,  $\Delta_{\text{fus}}H_1$ ,  $\Delta_{\text{fus}}C_{p,1}$ ,  $T_{\text{fus},1}$  and  $T$  stand for mole fraction, solute activity coefficient, enthalpy of fusion, difference in solute heat capacity between the liquid and solid at the melting

Table 4

Correlation of the solubility data (SLE) of {IL (1) + solvent (2)} mixtures, by means of the Wilson, UNIQUAC ASM and NRTL1 equations: values of parameters and measures of deviations

Solvent	Parameters			Deviations		
	Wilson	UNIQUAC ASM	NRTL1 <sup>a</sup>	$\sigma_T$ (K)		
	$g_{21} - g_{11}, g_{12} - g_{22}$ (J mol <sup>-1</sup> )	$\Delta u_{21}, \Delta u_{12}$ (J mol <sup>-1</sup> )	$\Delta g_{21}, \Delta g_{12}$ (J mol <sup>-1</sup> )	Wilson	UNIQUAC ASM	NRTL1
[(C <sub>8</sub> H <sub>17</sub> OCH <sub>2</sub> ) <sub>2</sub> IM][Tf <sub>2</sub> N]						
Ethanol	2537.5, 4296.3	713.64, -904.9	4377.6, 6775.9	2.92	8.60	2.79
Octan-1-ol	3057.0, 3331.4	377.6, -422.3	3032.8, 1353.4	2.25	4.66	2.75
[(C <sub>10</sub> H <sub>21</sub> OCH <sub>2</sub> ) <sub>2</sub> IM][Tf <sub>2</sub> N]						
Ethanol	-2808.3, 6601.6	1503.2, -1587.9	8273.0, -9418.9	1.55	2.65	2.12
Benzene	-556.4, 505.37	-	505.26, -578.7	0.84	-	0.84
[Pyr][BF <sub>4</sub> ]						
Ethanol	9231.8, 2513.1	1137.2, -1552.8	3415.2, 10200.5	3.66	9.52	1.62
Butan-1-ol	-	-	2235.1, 12653.0	-	-	1.84
Hexan-1-ol	29526.2, 1563.3	-	1360.7, 11835.1	2.50	-	2.34

<sup>a</sup> Calculated with the third non-randomness parameter  $\alpha = 0.3$ .

temperature (this value is unknown for the testing ILs), melting temperature of the solute (1) and measured equilibrium temperature, respectively. The procedure of correlation was described in our previous papers [35,39,42]. In this study the Wilson [45], UNIQUAC ASM [46] and the NRTL 1 [47] models were used to fit the solute activity coefficients,  $\gamma_1$  to the so-called correlation equations that describe the Gibbs excess free energy of mixing ( $G^{\text{Ex}}$ ) in some mixtures with alcohols and benzene.

The root-mean-square deviation of temperature [ $\sigma_T$  defined by Eq. (2)] was used as a measure of the goodness of the solubility correlation:

$$\sigma_T = \left( \frac{\sum_{i=1}^n ((T_i)^{\text{exp}} - (T_i)^{\text{cal}})^2}{n - 2} \right)^{1/2} \quad (2)$$

where  $n$  is the number of experimental points (including the melting point) and 2 is the number of adjustable parameters. The molar volumes  $V_m$  of pure component at 298.15 K for the hypothetical subcooled substances at 298.15 K, calculated from the group contribution method [48] were 295.9, 542.9, 607.3 and 325.3 cm<sup>3</sup> mol<sup>-1</sup> for [(C<sub>4</sub>H<sub>9</sub>OCH<sub>2</sub>)<sub>2</sub>IM][BF<sub>4</sub>], [(C<sub>8</sub>H<sub>17</sub>OCH<sub>2</sub>)<sub>2</sub>IM][Tf<sub>2</sub>N], [(C<sub>10</sub>H<sub>21</sub>OCH<sub>2</sub>)<sub>2</sub>IM][Tf<sub>2</sub>N] and [Pyr][BF<sub>4</sub>], respectively. The calculations were carried out by the use of the set of association parameters for alcohols described previously [42]. The Mecke–Kempter model for alcohol association was used. Table 4 lists the results of fitting the solubility curves for the chosen systems by these three equations together with the values of the parameter  $\alpha_{12}$ , a constant of proportionality similar to the non-randomness constant of the NRTL equations.

For the systems presented in this table, the description of solid–liquid equilibrium in alcohols given by the UNIQUAC ASM equation (assuming the association of alcohols) did not present any better results. It can be understood as a picture of a very complicated interaction between the molecules in the solution: it means that not only the association of alcohol molecules but also between alcohol–IL molecules and between

IL molecules exists. The average deviation for alcohols and benzene given by the NRTL1 model was  $\sigma_T < 2.8$  K, whilst by the UNIQUAC ASM model was  $\sigma_T < 6$  K. Parameters shown in Table 4 may be helpful for the describing activity coefficients for any concentration, temperature and for the description of ternary mixtures. They are also useful for the complete thermodynamic description of the solution.

## 5. Concluding remarks

Ionic liquids can be considered as highly ordered hydrogen-bonded substances and can have strong effects on chemical reactions and processes. Thus, the ability of IL to form hydrogen bonds or other possible interactions with potential solvents is an important feature of its behavior. Alcohols used in this work are also good hydrogen bond donors/acceptors, but not as good as ionic liquids. Greater interaction was observed for dialkoxy-salts than the alkoxy-salts. We believe this was due to the stronger interaction of two oxygen atoms with the solvent. Also the [Tf<sub>2</sub>N]<sup>-</sup> anion has shown better interaction with the solvent than the [BF<sub>4</sub>]<sup>-</sup> anion with the solvent. Therefore, the choice of anion can have huge effect on the phase behavior of ammonium and imidazolium ionic liquids.

In polar solvents like alcohols one can expect stronger interaction between unlike molecules than in alcohol, or IL itself. Clearly, hydrogen bonding, or  $n-\pi$ , or other interaction of cation, or anion of IL with solvent plays an important role in controlling liquid–liquid and solid–liquid phase behavior of ammonium and imidazolium-based ILs. However, the existence of the liquid–liquid phase equilibria in these mixtures is the evidence that the interaction between some of the IL and the solvent is not significant.

The binary mixture under study exhibited simple eutectic systems. The liquid–liquid phase diagrams for the mixtures under study exhibited upper critical solution temperatures (USCT). In many mixtures, the observations of USCT were limited by the boiling temperature of the solvent. Sometimes, it was

impossible to detect by the visual method the mutual solubility of IL with the solvent in the solvent rich phase. The spectroscopic or other techniques are necessary in the mentioned mixtures.

As compared to conventional organic solvents, ILs are much more complex solvents, capable of undergoing many types of interactions. Characterizing them with a single “polarity” term fails to describe the type and magnitude of individual interactions that make each IL unique.

### Acknowledgments

This research has been supported by the Polish Committee for Scientific Research (Grant 3 T09B 004 27). Author would like to thank students R. Bogel-Łukasik, B. Grzesiak and A. Wilk for co-operation and Prof. J. Pernak for the synthesis of the alkoxy-imidazolium and pyridinium samples.

### Appendix A. Supplementary data

Supplementary data associated with this article can be found, in the online version, at doi:10.1016/j.tca.2006.06.018.

### References

- [1] J. Holbrey, K.R. Seddon, *Clean Prod. Proc.* 1 (1999) 223.
- [2] L.C. Branco, J.N. Rosa, J.J.M. Ramos, C.A.M. Afonso, *Chem. Eur. J.* 8 (2002) 3671.
- [3] J.H. Werner, S.N. Baker, G.A. Baker, *Analyst* 128 (2003) 786.
- [4] S.N. Baker, G.A. Baker, F.V. Bright, *Green Chem.* 4 (2002) 165.
- [5] A.E. Bradley, C. Hardacre, J.D. Holbrey, S. Johnston, S.E.J. McMath, M. Nieuwenhuyzen, *Chem. Mater.* 14 (2002) 629.
- [6] S.V. Dzyuba, R.A. Bartsch, *Chem. Phys. Chem.* 3 (2002) 161.
- [7] J.L. Anthony, E.J. Maginn, J.F. Brennecke, *J. Phys. Chem. B* 105 (2001) 10942.
- [8] B. Wu, R.G. Reddy, R.D. Rogers, *Proceedings of the Solar Forum 2001, Solar Energy: The Power to Choose*, Washington, DC, USA, April 21–25, 2001.
- [9] P.A.Z. Suarez, S. Einloft, J.E.L. Dullius, R.F. De Souza, J. Dupont, *J. Chim. Phys.* 95 (1998) 1626.
- [10] G.W. Meindersma, A.J.G. Podt, A.B. de Haan, *Fuel Process. Technol.* 87 (2005) 59.
- [11] J. Fuller, R.T. Carlin, R.A. Osteryoung, *J. Electrochem. Soc.* 144 (1997) 3881.
- [12] M. Kosmulski, R.A. Osteryoung, M. Ciszowska, *J. Electrochem. Soc.* 147 (2000) 1454.
- [13] N. Papagerorgiou, Y. Athanassov, M. Armand, P. Bonhôte, H. Pettersson, A. Azam, M. Grätzel, *J. Electrochem. Soc.* 143 (1996) 3099.
- [14] U. Schröder, J.D. Wadhawan, R.G. Compton, F. Marken, P.A.Z. Suarez, C.S. Consorti, R.F. De Souza, J. Dupont, *J. New J. Chem.* 24 (2000) 1009.
- [15] D.R. McFarlane, J. Sun, J. Golding, P. Meakin, M. Forsyth, *Electrochem. Acta* 45 (2000) 1271.
- [16] J.G. Huddleston, H.D. Willauer, R.P. Swatloski, A.E. Visser, R.D. Rogers, *Chem. Commun.* 1765 (1998).
- [17] S. Dai, Y.H. Ju, C.E. Barnes, *J. Chem. Soc., Dalton Trans.* 1201 (1999).
- [18] A.E. Visser, R.P. Swatloski, R.D. Rogers, *Green Chem.* 2 (2000) 1.
- [19] W. Arlt, M. Seiler, G. Sadowski, H. Frey, H. Kautz, *DE Patent* 10160518.8.
- [20] M. Krummen, P. Wasserscheid, J. Gmehling, *J. Chem. Eng. Data* 47 (2002) 1411.
- [21] N. Deenadayalu, T.M. Letcher, P. Reddy, *J. Chem. Eng. Data* 50 (2005) 105.
- [22] T.M. Letcher, A. Marciniak, M. Marciniak, U. Domańska, *J. Chem. Thermodyn.* 37 (2005) 1327.
- [23] T.M. Letcher, M. Marciniak, A. Marciniak, U. Domańska, *J. Chem. Eng. Data* 50 (2005) 1294.
- [24] R. Kato, J. Gmehling, *Fluid Phase Equilib.* 226 (2004) 37.
- [25] A. Heintz, D.V. Kulikov, S.P. Verevkin, *J. Chem. Eng. Data* 46 (2001) 1526.
- [26] K.N. Marsh, A. Deev, A.C.-T. Wu, E. Tran, A. Klamt, *Kor. J. Chem. Eng.* 19 (2002) 357.
- [27] V. Najdanovic-Visak, J.M.S.S. Esperanca, L.P.N. Rebelo, M.N. da Ponte, H.J.R. Guedes, K.R. Seddon, R.F. de Souza, J. Szydlowski, *J. Phys. Chem. B* 107 (2003) 12797.
- [28] A. Heintz, J.K. Lehmann, C. Wertz, *J. Chem. Eng. Data* 48 (2003) 472.
- [29] J.M. Crosthwaite, S.N.V. Akai, E.J. Maginn, J.F. Brennecke, *J. Phys. Chem. B* 108 (2004) 5113.
- [30] C.-T. Wu, K.N. Marsh, A.V. Deev, J.A. Boxall, *J. Chem. Eng. Data* 48 (2003) 486.
- [31] U. Domańska, A. Marciniak, *J. Chem. Eng. Data* 48 (2003) 451.
- [32] U. Domańska, A. Marciniak, *J. Phys. Chem. B* 108 (2004) 2376.
- [33] J.M. Crosthwaite, S.N.V. Aki, E.J. Maginn, J.F. Brennecke, *Fluid Phase Equilib.* 228–229 (2005) 303.
- [34] U. Domańska, A. Marciniak, *J. Chem. Thermodyn.* 37 (2005) 577.
- [35] U. Domańska, L. Mazurowska, *Fluid Phase Equilib.* 221 (2004) 73.
- [36] U. Domańska, A. Pobudkowska, F. Eckert, *Green Chem.* 8 (2006) 268.
- [37] U. Domańska, A. Pobudkowska, F. Eckert, *J. Chem. Thermodyn.* 38 (2006) 685.
- [38] U. Domańska, E. Bogel-Łukasik, R. Bogel-Łukasik, *J. Phys. Chem. B* 107 (2003) 1858.
- [39] U. Domańska, E. Bogel-Łukasik, *Ind. Eng. Chem. Res.* 42 (2003) 6986.
- [40] U. Domańska, A. Marciniak, R. Bogel-Łukasik, *ACS Symposium Series Ionic Liquids*, ACS, New York, USA, 2005.
- [41] U. Domańska, R. Bogel-Łukasik, *J. Phys. Chem. B* 109 (2005) 12124.
- [42] U. Domańska, R. Bogel-Łukasik, *Fluid Phase Equilib.* 233 (2005) 220.
- [43] J. Pernak, A. Olszówka, R. Olszewski, *Polish J. Chem.* 77 (2003) 179.
- [44] J. Pernak, K. Sobaszekiewicz, J. Foksowicz-Flaczyk, *Chem. Eur. J.* 10 (2004) 3479.
- [45] G.M. Wilson, *J. Am. Chem. Soc.* 86 (1964) 127.
- [46] I. Nagata, *Fluid Phase Equilib.* 19 (1985) 153.
- [47] J. Nagata, Y. Nakamiya, K. Katoh, J. Koyabu, *Thermochim. Acta* 45 (1981) 153.
- [48] A.F.M. Barton, *CRC Handbook of Solubility Parameters*, CRC Press Inc., Boca Raton, FL, USA, 1985, p. 64.